

Stochastic resonance in the mechano-electrical transduction of hair cells

John F. Lindner,¹ Matthew Bennett,² and Kurt Wiesenfeld²

¹Physics Department, The College of Wooster, Wooster, Ohio 44691, USA

²Center for Nonlinear Science and School of Physics, Georgia Institute of Technology, Atlanta, Georgia 30332, USA

(Received 23 April 2005; revised manuscript received 8 July 2005; published 7 November 2005)

In transducing mechanical stimuli into electrical signals, at least some hair cells in vertebrate auditory and vestibular systems respond optimally to weak periodic signals at natural, nonzero noise intensities. We understand this *stochastic resonance* by constructing a faithful mechanical model reflecting the hair cell geometry and described by a nonlinear stochastic differential equation. This *Langevin* description elucidates the mechanism of hair cell stochastic resonance while supporting the hypothesis that noise plays a functional role in hearing.

DOI: [10.1103/PhysRevE.72.051911](https://doi.org/10.1103/PhysRevE.72.051911)

PACS number(s): 87.19.Rr, 87.10.+e, 05.45.-a

I. INTRODUCTION

The vertebrate ear nonlinearly transduces mechanical energy into electrical impulses enabling us to sense sounds and movements whose intensity varies a millionfold. Although still incompletely understood, such mechano-electrical transduction is especially amenable to physical analysis [1,2]. Hair cells are the key elements in both auditory and vestibular transductions, and they have been the subject of intense study, including current research elucidating the chemical constituents of some of their structural elements [3–5]. Recent modeling [6,7] suggests that feedback mechanisms may self-tune some hair cells to an oscillatory instability enabling them to actively amplify signals. However, other experiments [8–10] suggest that a passive amplification mechanism involving noise and nonlinear dynamics may also be involved. While the cochlea's outer hair cell bundles are attached to an overarching membrane, its inner hair cell bundles are free to experience significant Brownian motion, and the resulting noisy environment may actually *enhance* their sensitivity. Although dramatically outnumbered by outer hair cells, inner hair cells are responsible for most of the auditory information sent to the brain—and seem to be designed with noise in mind.

Stochastic resonance [11,12] is a noise-enhanced response to a weak periodic signal that has been observed in many nonlinear physical and biological systems. Experiments have demonstrated stochastic resonance in the vertebrate auditory system [13] and in frog saccular hair cells [8–10]. The latter experiments have been modeled [14] theoretically using time and temperature-dependent transition rates for a bistable potential representing open and closed transduction states. In this paper, we present a nonlinear Langevin model of hair cell stochastic resonance in these experiments. The model directly reflects the mechanics of the hair cell geometry. It is conceptually simple, although analytically difficult. (It incorporates, for example, two independent colored noise sources). Consequently, we investigate the model numerically. With physiologically plausible parameters, it successfully reproduces the salient features of the experiments while simultaneously enabling the testing of further hypotheses.

II. HAIR CELL MODEL

Figure 1 is a schematic diagram of a hair cell, whose stereocilia pivot in unison with the motion of the surrounding fluid, thereby opening and closing ion channels in the cilia walls, the first stage in sending electrical impulses to the brain. The transduction is so quick that it must be directly mechanical [15]. The canonical model [16] involves a mechanical linkage applying tension to a transduction channel gate via a tether connecting the top of one cilium to the side of its taller neighbor. Because the shearing induced by the pivoting of the cilia does not break the tether, and because the channel gate can rattle open and closed when the cilia are held fixed [17], the mechanical linkage must be elastic. Cutting the tether eliminates the tension on the gate, and hence the elastic element must either be the tether or be in series with it [18]. The gate itself exhibits a positive restoring force for large displacements but negative restoring force for small displacements [19], and so we model it with a bistable potential, whose minima correspond to open and closed configurations, which probably reflect two different conformations of a protein gate molecule.

III. LANGEVIN DESCRIPTION

We idealize the stereocilia as a bundle of two parallel rods that pivot with the motion of fluid in the ear, sinusoidally in response to acoustic waves and noisily in response to Brownian motion, so that the horizontal displacement of the bundle tip is

$$x_B[t] = \epsilon \sin[2\pi ft] + \sigma_B \xi_B[t], \quad (1)$$

where the Gaussian noise $\xi_B[t]$ is exponentially correlated,

$$\langle \xi_B[t] \xi_B[t + \tau] \rangle = e^{-|\tau|/\tau_B}, \quad (2)$$

because the fluid viscosity damps the higher frequencies. (The resulting position fluctuation spectrum is somewhat different from the spectrum of a hair cell model that spontaneously oscillates [7], but our model operates in a bistable rather than an oscillatory regime.)

We assume the gate has length L , moment arm $\rho \ll L$, and swings through a large angle θ as the rods tilt through a

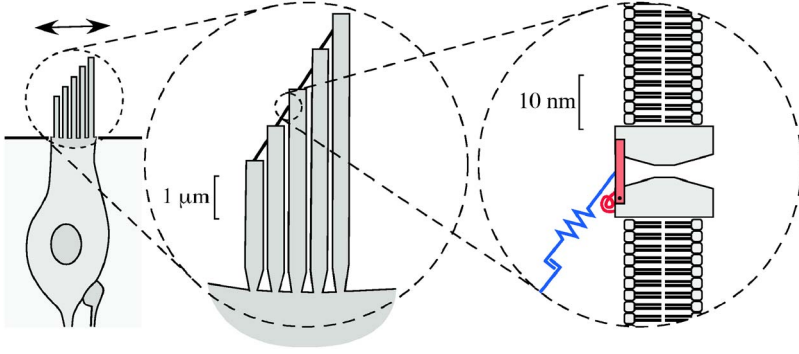


FIG. 1. (Color online) Simplified cross sections of an inner hair cell (left), bundle of pivoting stereocilia with tip link tethers (center), and ion channel with a schematic gate (right). Motion is primarily in the plane of the figure.

small angle φ , as shown schematically in Fig. 2. The gate vector $\vec{\rho} = \{-\rho \sin[\theta - \varphi], \rho \cos[\theta - \varphi], 0\}$, and the coordinates $\vec{r}_1 = \{d, 0, 0\}$, $\vec{r}_2 = \vec{r}_1 + \{H \sin \varphi, H \cos \varphi, 0\}$, $\vec{r}_3 = \vec{r}_2 + \vec{\rho}$, and $\vec{r}_4 = \{h \sin \varphi, h \cos \varphi, 0\}$. Hence the link vector $\vec{l} = \vec{r}_4 - \vec{r}_3$. We model the tip link as an elastic tether that pulls the gate with a force $\vec{F} = k(l - l_0)\hat{l}$, where l_0 is the equilibrium length of the link, and \hat{l} is a unit vector along the link pointing away from the gate. This produces a torque $\vec{\tau}_L = \vec{\rho} \times \vec{F}$ whose magnitude is a trigonometric function of both θ and φ .

The tip link tethers are not springs, as experiments have observed them to slacken [20,21] for negative displacements. We represent this in Fig. 1 by the decoupler in series with the spring and, in the simulation, we multiply the tether force by the unit step function $\Theta[l - l_0]$, if necessary, to ensure that the tether only pulls and never pushes.

We model the gate dynamics with the asymmetric quartic (tilted double well) potential

$$U_G[\theta] = 4U_0 \left(-\frac{1}{2} \left(\frac{\theta - c}{c} \right)^2 + \frac{1}{4} \left(\frac{\theta - c}{c} \right)^4 \right) + A(\theta - c), \quad (3)$$

where the constants U_0 , c , and A determine the potential height, radius, and asymmetry. The corresponding gate torque is $\tau_G[\theta] = -U'_G[\theta]$.

The channel gate is probably a protein with a typical mass of tens to hundreds of kilodaltons, where 1 kDa $\sim 10^3$ a.m.u. $\sim 10^{-24}$ kg $= 10^{-15}$ μg. Its tiny size makes its inertia negligible compared to the viscosity of the ambient fluid. Hence, we assume the Langevin equation of motion

$$\Gamma \dot{\theta} = \tau_G[\theta] + \tau_L[\theta, \varphi] + \sigma_G \xi_G[t], \quad (4)$$

where Γ is the angular friction coefficient of the gate, and the overdot indicates time differentiation. The bundle tip displacement x_B of Eq. (1) drives the Langevin equation via the relation $\varphi \sim x_B/H$ from Fig. 2. The additional stochastic term $\xi_G[t]$ models gate thermal fluctuations, and we choose the rms gate noise σ_G such that the ratio of gate opened time to the gate closed time is the Boltzmann factor

$$t_o/t_c = e^{-\Delta U/kT}, \quad (5)$$

where T is the temperature, and ΔU is the potential energy difference between the opened and closed states when the stereocilia are fixed at the equilibrium position $\varphi = 0$. We take the transduction current to be proportional to $\text{sgn}[\theta - c]$, so

that it is linearly dependent on the gate angle θ , but binary filtered to obtain a stylized version of the switchlike response of an actual channel gate.

IV. TYPICAL PARAMETERS

We adopt the length, time, and mass scales of 1 nm $= 10^{-9}$ m, 1 ms $= 10^{-3}$ s, and 1 μg $= 10^{-9}$ kg. In our computer simulations, we set these quantities to unity to preserve precision. In these units, 1 zJ $= 10^{-21}$ J $= 1$ μg nm²/ms² and 1 yW $= 10^{-24}$ W $= 1$ μg nm²/ms are also unity, and room temperature corresponds to $kT \sim (1/40)eV \sim 4$ zJ.

The viscosity and density of the endolymph, the fluid bathing the hair cells, is similar to that of water at room (or body) temperature [22,23]. In particular, the endolymph's viscosity is $\eta \sim 1$ cP $= 10^{-3}$ Pa s $= 10^{-6}$ MPa ms $= 10^{-6}$ yW/nm³. Recalling that $L \geq \rho$ is the gate length, if v is a characteristic speed, then $\gamma v = F \sim \eta(v/L)L^2$ and the linear friction coefficient $\gamma \sim \eta L$. Similarly, if ω is a characteristic angular speed, then $\Gamma v/L \sim \Gamma \omega = \tau \sim LF = L\gamma v$ and the angular friction coefficient $\Gamma \sim \gamma L^2 \sim \eta L^3$. Thus, if $L \sim 10$ nm, then $\gamma \sim 10^{-5}$ yW/nm² and $\Gamma \sim 10^{-3}$ yW. (The model is actually insensitive to the precise value of Γ .)

Physiologically plausible parameters include a potential energy barrier height U_0 of a few kT and a barrier radius c of a radian or two (corresponding to the range of swing of the gate). Hair bundle heights and separation H , h , and d are micron sized with a geometric gain $g = (H - h)/H$ of about a

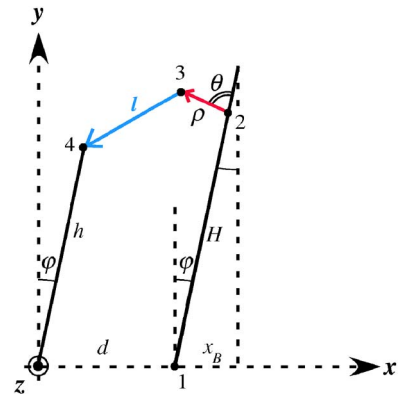


FIG. 2. (Color online) Schematic diagram exaggerates the stereocilia tilt angle φ and the transduction channel gate moment arm ρ but not the gate angle θ . In reality, $\varphi \ll 1$ and $\rho \ll H - h < d$.

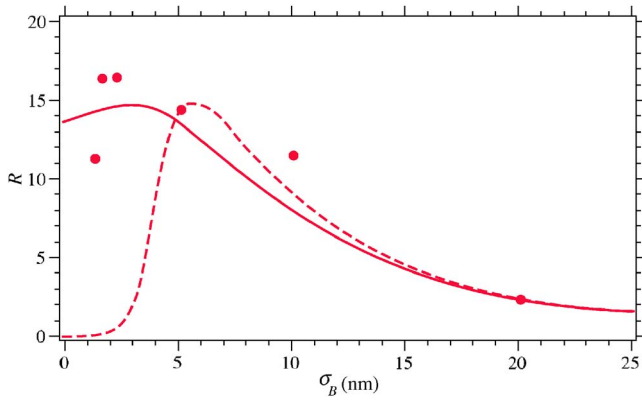


FIG. 3. (Color online) Signal-to-noise ratio R as a function of bundle tip r.m.s. noise σ_B for the benchmark model parameters of Table I with (solid line) and without (dashed line) gate noise σ_G , superimposed on biological data from Ref. [8] (dots). The gate noise shifts the peak to lower bundle tip noise and broadens it. The model response at 2–3 nm is 5–10 % better than at zero.

tenth [6,7]. To compare with experiment, the signal amplitude ϵ is a few nanometers and the signal frequency f is about a kilohertz. Typical stereocilia Brownian motion rms noise σ_B is a few nanometers at the tip with correlation time τ_B of about a millisecond (due to viscous drag and corresponding to the experimental kilohertz low-pass filter [8]). The link stiffness is a few piconewtons per nanometer [21], and its equilibrium length is about half a micron. We estimate the gate moment arm to be a few nanometers.

V. ANALYSIS

We numerically integrate Eq. (4) using the algorithm of Fox *et al.* [24] with an integration time step dt of about ten nanoseconds. With typical parameters and the tip link tether broken, the effective potential U for the combined gate and link is many kT deep, corresponding to the gate being “locked” closed, and this is in good agreement with experiment. However, with the link attached and sinusoidally driven, the effective potential is relatively shallow, bistable, and dynamic, rocking back and forth. The link torque is positive at all gate angles, meaning the link is always under tension, and fluctuates in time, but more so at the closed position than at the open, as the link is stretched more when the gate is closed. When the gate opens, the tension in the link drops. An angular probability distribution reveals that the swinging gate is mostly open or closed and rarely in between, like a screen door flapping in the breeze.

We spectrally analyze the numerically generated and binary filtered time series $\text{sgn}[\theta - c]$ with a temporal sampling of $\Delta t = 2^{-10}$ ms ~ 1 μ s and a frequency resolution of $\Delta f = 2^{-8}$ kHz ~ 3.9 Hz. We Welch window the time series to reduce bin leakage, average 2^8 spectra, and find a sharp frequency peak of height S at the drive frequency superimposed on a Lorentzian background of height N . We compute the signal-to-noise ratio $R = (S/N - 1)/G \geq 0$, where the processing gain $G = 5/6$ accounts for the Welch window scaling of narrow-band peaks. Figure 3 shows the signal-to-noise ratio

TABLE I. Benchmark model parameters.

Quantity	Symbol	Value(s)
Signal frequency	f	0.3 kHz
Signal amplitude	ϵ	2 nm
Rod separation	d	500 nm
Rod height tall	H	3000 nm
Rod height short	h	2700 nm
Tip link stiffness	k	8 pN/nm
Tip link equilibrium length	l_0	580 nm
Bundle tip noise r.m.s.	σ_B	0–25 nm
Bundle tip noise correlation time	τ_B	1 ms
Gate friction	Γ	0.001 yW
Gate potential height	U_0	12 zJ
Gate potential half-width	c	$\pi/4$ rad
Gate potential asymmetry	A	45 pN nm
Gate moment arm	ρ	2 nm
Gate noise r.m.s.	σ_G	7 pN nm
Gate noise correlation time	τ_G	1 ms

R as a function of rms noise σ_B for one set of plausible parameters, those of the “benchmark model” listed in Table I. The stochastic resonance peak at a few nanometers is in good agreement with the biological data [8].

The mechanical connectivity of the model interrelates the parameters in subtle ways. In addition, while the location of the stochastic resonance is robust with respect to changes in some of the parameters, such as the friction coefficient Γ , it is sensitive to changes in other parameters, such as the tip link equilibrium length, which tension the tip link tether. In fact, hair cells have fast and slow adaptation mechanisms, reacting in less than a millisecond to tens of milliseconds, that continually adjust this tension [15,25]. For example, in slow adaptation, the hair cell geometry is dynamic because the channel gates are connected to myosin motors that climb and slide along actin filaments in the stereocilia.

To further test the model, we consider the hair cell’s displacement-response curve, a plot of the channel gate open probability P_o versus the mean bundle tip displacement $\langle x_B \rangle$ in the absence of a sinusoidal signal but in the presence of the background noise characteristic of stochastic resonance. In the benchmark model, the displacement-response curve resembles a sigmoid that naturally opens over a scale of ~ 1 nm. In actual experiments, the hair cell opens over ~ 100 nm. How can we reconcile these two results? Inspired by the emerging understanding of hair cell adaptation, we extend the model by incorporating the retensioning of the tip link tether, which we simply accomplish by allowing the tether’s equilibrium length to change with the time-averaged bundle tip location $\langle x_B \rangle \sim H\langle \varphi \rangle$ according to

$$l_0 \rightarrow l_0 + r\langle x_B \rangle, \quad (6)$$

where r is a dimensionless rate-of-change parameter. Since normally, in the signal-to-noise experiments, the time-averaged bundle tip location vanishes $\langle x_B \rangle = 0$, this does not

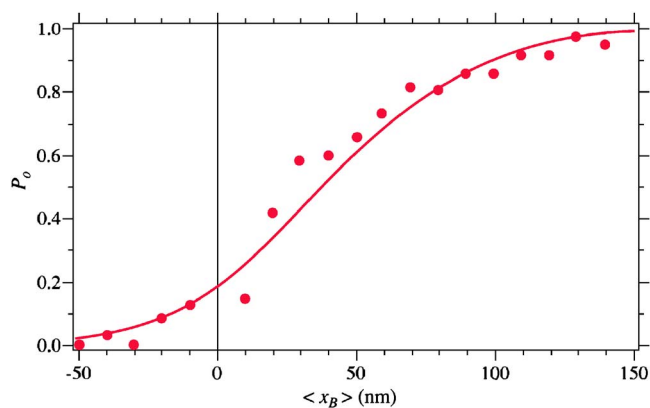


FIG. 4. (Color online) Near stochastic resonance, open probability P_o versus mean bundle tip location $\langle x_B \rangle$ (solid line) superimposed on biological data from Ref. [8] (dots).

affect the previous results, but it does dramatically broaden the displacement-response curve, as seen in Fig. 4, where a modest rate-of-change of $r \sim 0.08$ produces good agreement with experiment [8]. (Note that the time scale for the retensioning of the tip link tether is slow compared to the oscillation time scale of Fig. 3 but fast compared to the data acquisition time of Fig. 4.)

VI. CONCLUSIONS

In summary, the Langevin model captures the main features of hair cell stochastic resonance with physiologically plausible parameters. While refinements of the model and

further experiments may be needed to optimize the model parameters, the current correspondence between simulation and experiment strengthens our confidence in the biophysics of the phenomenon and in the suggestion that noise in the inner ear can be sometimes helpful rather than always harmful. The Langevin model vividly demonstrates one way the vertebrate ear may have evolved to exploit noise to detect faint sounds, and we suggest that this mechanism is complementary to active amplification schemes. The fact that both gate noise and bundle noise are essential to get the physics right supports a hypothesized [8,14] division of duty between the outer hair cells, whose stereocilia are coupled to an overarching membrane, and the inner hair cells, whose stereocilia are free: The former may actively amplify signals while the latter may exploit bundle (and gate) noise to boost signal detection. Finally, the Langevin model can be generalized and employed in diverse directions, such as attacking the open question of whether the tip link tether itself is the gating spring or whether it is merely in series with the gating spring [18]; investigating the possibility of hair cell array-enhanced stochastic resonance [26–28]; and exploring the advantage (or not) of having a gate at each end of the tether. Such questions remind us that deep inside the vertebrate ear is a simple but ingenious mechanical system fine-tuned to exploit ambient noise to detect the slightest movement or faintest whisper.

Acknowledgments

J.F.L. thanks The College of Wooster for making possible his sabbatical at Georgia Tech. This work was supported in part by ONR Grant No. N00014-99-1-0592. We thank Fernán Jaramillo for helpful discussions.

-
- [1] T. Duke and F. Jülicher, *Phys. Rev. Lett.* **90**, 158101 (2003).
 - [2] T. M. Squires, *Phys. Rev. Lett.* **93**, 198106 (2004).
 - [3] J. Siemens *et al.*, *Nature (London)* **428**, 950 (2004).
 - [4] C. Söllner *et al.*, *Nature (London)* **428**, 955 (2004).
 - [5] D. P. Corey *et al.*, *Nature (London)* **432**, 723 (2004).
 - [6] A. Vilfan and T. Duke, *Biophys. J.* **85**, 191 (2003).
 - [7] B. Nadrowski, P. Martin, and F. Jülicher, *Proc. Natl. Acad. Sci. U.S.A.* **101**, 12195 (2004).
 - [8] F. Jaramillo and K. Wiesenfeld, *Nat. Neurosci.* **1**, 384 (1998).
 - [9] F. Jaramillo and K. Wiesenfeld, *Chaos, Solitons Fractals* **11**, 1869 (2000).
 - [10] A. Indresano, J. Frank, P. Middleton, and F. Jaramillo, *J. Assoc. Res. Otolaryngol.* **4**, 363 (2003).
 - [11] L. Gammaitoni, P. Hänggi, P. Jung, and F. Marchesoni, *Rev. Mod. Phys.* **70**, 223 (1998).
 - [12] P. Hänggi, *ChemPhysChem* **3**, 285 (2002).
 - [13] F. Moss, in *Contemporary Problems in Statistical Physics*, edited by G. H. Weiss (SIAM, Philadelphia, 1994), p. 205.
 - [14] M. Bennett, K. Wiesenfeld, and F. Jaramillo, *Fluct. Noise Lett.* **4**, L1 (2004).
 - [15] P. G. Gillespie and J. L. Cyr, *Annu. Rev. Physiol.* **66**, 521 (2004).
 - [16] D. P. Corey and A. J. Hudspeth, *J. Neurosci.* **3**, 962 (1983).
 - [17] W. M. Roberts, J. Howard, and A. J. Hudspeth, *Annu. Rev. Cell Biol.* **4**, 63 (1988).
 - [18] D. P. Corey and M. Sotomayor, *Nature (London)* **428**, 901 (2004).
 - [19] P. Martin, A. D. Mehta, and A. J. Hudspeth, *Proc. Natl. Acad. Sci. U.S.A.* **97**, 12026 (2000).
 - [20] J. A. Assad and D. P. Corey, *J. Neurosci.* **12**, 3291 (1992).
 - [21] J. Howard and A. J. Hudspeth, *Neuron* **1**, 189 (1988).
 - [22] T. M. Squires, M. S. Weidman, T. C. Hain, and H. A. Stone, *J. Biomech.* **37**, 1137 (2004).
 - [23] J. P. Bronzino, *The Biomedical Engineering Handbook* (CRC Press, Boca Raton, 2000).
 - [24] R. F. Fox, I. R. Gatland, R. Roy, and G. Vemuri, *Phys. Rev. A* **38**, 5938 (1988).
 - [25] R. A. Eatock, *Annu. Rev. Neurosci.* **23**, 285 (2000).
 - [26] P. Jung, U. Behn, E. Pantazelou, and F. Moss, *Phys. Rev. A* **46**, R1709 (1992).
 - [27] J. F. Lindner, B. K. Meadows, W. L. Ditto, M. E. Inchiosa, and A. R. Bulsara, *Phys. Rev. Lett.* **75**, 3 (1995).
 - [28] J. J. Collins, C. C. Chow, and T. T. Imhoff, *Nature (London)* **376**, 236 (1995).